# Analyst

**COMMUNICATION**

# A solution-based nano-plasmonic sensing technique by using gold nanorods

**Fu Han Ho,**[*a] **Yung-Han Wu,**[b] **Masaki Ujihara**[a] **and Toyoko Imae**[*ac]

**We have successfully demonstrated a novel sensing technique for monitoring the variation of solution concentrations and measuring the effective dielectric constant in a medium by means of an ultra-small and label-free nanosensor, the mechanism of which is based on the localized surface plasmon resonance (LSPR) of gold nanorods. The nanorods are fabricated in a narrow size distribution, which is characterized by transmission electron microscopy and optical absorption spectroscopy. In addition, we employ a simple analytical calculation to examine the LSPR band of the absorption spectrum, which provides excellent consistency with aspect ratio. The plasmonic sensing is performed by detecting the diffusion process and saturation concentration of hexadecyltrimethylammonium bromide in water, and tracing the effective dielectric constants of the medium simultaneously. This promising sensing and analytical technique can be easily used for investigating the nano-scale variations of mixing or reaction process in a micro/nanofluidic channel or the biological interaction in the cytoplasm of the cell.**

## Introduction

Metallic nanoparticles have been extensively studied for over 100 years due to their unique optical properties.[1,2] Fundamentally, electromagnetic wave incident on the metallic nanoparticles induces a collective oscillation of free electrons at a resonant frequency, a phenomenon known as localized surface plasmon resonance (LSPR), which depends on the size, shape and composition of the nanoparticle, and also sensitively relates to the refractive index of the surrounding environment.[3,4] LSPR can be determined and measured through an extinction spectrum (scattering and absorption) at visible and near-infrared (NIR) wavelengths and in particular the peak wavelength $\lambda_{max}$. With spectral tunability[5,6] and strong enhancement of the local electric fields,[7,8] extensive advances have been developed in LSPR-based nanodevices with new integrated functionalities for future chemical and biological sensing techniques. This nano-scaled, size-based, and label-free nanosensor by using a single nanoparticle

*[a]Graduate Institute of Applied Science and Technology, National Taiwan University of Science and Technology, Taipei 10607, Taiwan, R.O.C. E-mail: fuhanho@mail.ntust.edu.tw*
*[b]Department of Materials Science and Engineering, National Taiwan University of Science and Technology, Taipei 10607, Taiwan, R.O.C.*
*[c]Department of Chemical Engineering, National Taiwan University of Science and Technology, Taipei 10607, Taiwan, R.O.C. E-mail: imae@ mail.ntust.edu.tw*

assists optical transduction of tiny environmental changes or single binding event at their surface into optical signals.[9–11] The sensing range of LSPR around a single nanoparticle is highly confined within tens of nanometres,[12–15] and the detection capability evanescently decays above the surface. The advantages of transducer miniaturization and field confinement are that sample volumes can be greatly reduced or the implantation can be easily achieved in the micro/nanofluidic channel and cell.[16–18]

Gold nanorods, anisotropic and elongated nanoparticles, have well-defined optical properties and have attracted much attention in biomedical applications such as biosensing,[19] bioimaging,[20] and photothermal therapy.[21] A gold nanorod has two LSPR bands, namely, the transverse band and the longitudinal band, corresponding to electron oscillations in the short and long axes of the nanorod, respectively. The longitudinal LSPR band expresses strong scattering and absorption and can be tuned from visible to NIR region by adjusting the aspect ratio (length to width) of the nanorod. The longitudinal plasmon resonances of gold nanorods are highly polarization-dependent and have a linewidth significantly narrower than that of other gold nanoparticles. The longitudinal absorption band is extremely sensitive to the changes in the dielectric properties of the surroundings, including solvents, adsorbates, and the interparticle distance of the gold nanorods. The advantage of this sharp, polarized NIR resonance could enable multiplexed biological sensing and biomedical imaging through multi-spectral and polarization-sensitive detection.[22] Significant biomedical applications could be achieved when LSPR bands are tuned to the NIR region, where tissue is relatively transparent.

In this study, we report a novel sensing technique for monitoring the variations of solution concentrations, and measuring the effective dielectric constants in medium by means of an ultra-small and label-free sensor with gold nanorods. The nanorods are synthesized with narrow distribution for each different size, which is examined by transmission electron microscopy (TEM) and optical absorption spectroscopy. We introduce a simple analytical model to calculate the LSPR band of the absorption spectrum, which provides excellent fitting curves with a defined aspect ratio. The plasmonic sensing is verified by detecting the different phenomena of a chemical compound in water. Compared with the biological binding event, the phenomenon in a medium is more complicated for analysis. From the experimental results, the diffusion, absorption and saturation processes of hexadecyltrimethylammonium bromide ($C_{16}TAB$) both in the water and on the nanorod are simultaneously monitored by the peak shifts of absorption spectrum. In addition, the effective dielectric constants of the $C_{16}TAB$ solution with different concentrations in the

optical regime are calculated. This information will provide a useful guidance for the sensible design and analysis of LSPR biosensors in medium or biological specimens.

## Materials and methods

### Preparation of gold nanorods

All chemicals were commercially available and used without further purification. Ultrapure water (>18.2 MΩ) was used throughout all the experiments. Gold nanorods were prepared at 30 °C by a seed-mediated method.[23,24] A seed solution was prepared as follows: a freshly prepared aqueous solution (0.8 cm³) of 0.01 M NaBH₄ was added dropwise into a mixture of yellow aqueous solution (3.7 cm³) of 1 mM HAuCl₄ and an aqueous solution (11.3 cm³) of 0.13 M C₁₆TAB with mild stirring. The preparation of a growth solution is as follows: an aqueous solution (0.8 cm³) of 0.01 M AgNO₃ and an aqueous solution (0.75 cm³) of 0.1 M ascorbic acid were mixed with a yellow aqueous solution (25 cm³) of 1 mM HAuCl₄ and 0.13 M C₁₆TAB under mild stirring. At the next step, the brown seed solution was mixed with the transparent growth solution, and the mixture was kept for at least 3 h, where a violet solution was obtained.

In order to characterize the particle size, the morphology of gold nanorods was visualized by using TEM (Hitachi H-7000, Japan). For the sample preparation, the dispersion of gold nanorods was first treated with dialysis to remove the excess C₁₆TAB, after the filtration removal of crystallized C₁₆TAB at 4 °C. Next, it was dropped onto the copper grid and dried out at the room temperature. The dialysis-treated dispersion was also used for the measurement of UV absorption spectrum in a 1 cm quartz cell on the UV spectrometer (Hitachi F-7000, Japan).

### Theoretical calculation

To investigate the LSPR effect of a gold nanorod in the suspension, such as the identification of the particle size or aspect ratio from the absorption spectrum, theoretical calculations based on Mie theory with some modifications were applied. The dielectric constant $\varepsilon(\omega)$ at frequency $\omega$, derived from Drude's model, including size effect is as follows:[25]

$$\varepsilon(\omega) = \varepsilon_{\exp}(\omega) + \frac{\omega_p^2}{\omega^2 + i\Gamma_{\text{bulk}}\omega} - \frac{\omega_p^2}{\omega^2 + i\Gamma\omega}$$

where $\varepsilon_{\exp}(\omega)$ is dielectric constant obtained from the experiments, and $\omega_p$ is plasma frequency.[26] The damping constant $\Gamma$ with the size effect was given by

$$\Gamma = \Gamma_{\text{bulk}} + Av_F/r_1$$

where $\Gamma_{\text{bulk}}$ is the damping constant for the bulk, $r_1$ is the sectional radius of the rod, $A$ is a constant (nearly equal to unity), and $v_F$ is Fermi velocity. Necessary parameters can be found in the literature.[25,26] For a nanorod, the Gans modification of Mie theory for elongated nanoparticles within the dipole approximation assumed that the absorption of incident energy was mainly caused by electric dipole oscillation of the nanoparticles. According to Gans theory,[27] the extinction coefficient $\gamma$ was

$$\gamma = \frac{2\pi N V \varepsilon_m^{3/2}}{3\lambda} \sum_j \frac{\left(1/P_j^2\right)\varepsilon_2}{\left(\varepsilon_1 + \frac{1-P_j}{P_j}\varepsilon_m\right)^2 + \varepsilon_2^2}$$

where $N$ is the number of particles per unit volume, $V$ is the volume of each particle, $\varepsilon_m$ is the dielectric constant of the surrounding medium, $\lambda$ is the wavelength of the light, and $\varepsilon_1$ and $\varepsilon_2$ are the real and complex part of the material dielectric constant $\varepsilon(\omega)$. $P_j$ is the depolarization factor for the three axes $A$, $B$, $C$ of the rod ($A > B = C$). They were derived as follows:

$$P_A = \frac{1-e^2}{e^2}\left[\frac{1}{2e}\ln\left(\frac{1+e}{1-e}\right) - 1\right],$$

and

$$P_B = P_C = \frac{1-P_A}{2}$$

where $e = \sqrt{1 - \left(\frac{B}{A}\right)^2} = \sqrt{1 - \left(\frac{1}{R}\right)^2}$, and $R$ is the aspect ratio of gold nanorod.

## Results and discussion

### Characterization of nanorods with a single size

Fig. 1(a) shows a TEM micrograph of gold nanorods. The size of the nanorod is mostly 36 nm in length and 10 nm in diameter, and then the aspect ratio is about 3.6. To examine the uniformity of gold nanorods, the UV absorption spectroscopy can be used for the characterization of whole dispersion. Fig. 1(b) shows UV spectra of experimental (solid line) and theoretical (dashed line) results. The spectrum has two main bands, 520 nm and 762 nm, in the visible and NIR region, respectively. The strong peak of longer wavelength at 762 nm indicates the longitudinal plasmon band, which is due to excitation along the nanorod length. Its observed band position provides good agreement with the theoretical calculation at the condition of the aspect ratio 3.6. The LSPR spectral full-width at half-maximum (FWHM) of 100 nm is larger than theoretical value of 60 nm, since the broadening is related to the size distribution. The weak band of shorter wavelength at 520 nm is the transverse plasmon band which results from the excitation across the nanorod diameter and is similar to plasmon resonances in spherical gold colloid.
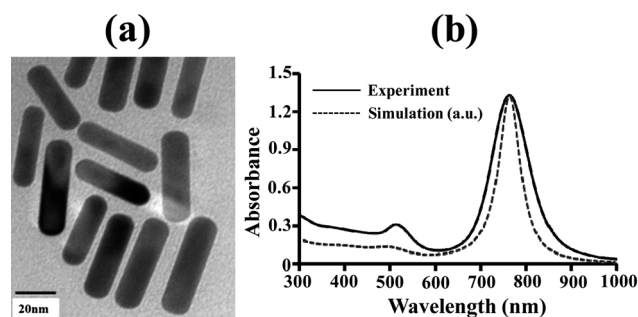


**Fig. 1** (a) A TEM micrograph of gold nanorods. (b) Absorption spectra of the colloidal gold nanorods with an aspect ratio of 3.6. The solid line is the experimental result, and the dashed line is the simulation result.

## Identification of nanorods with two different sizes

The sharp and tunable absorption band of a gold nanorod at the longer wavelength enables the unique "multiplexing" advantage to be realized because nanorods with different aspect ratios could be easily fabricated. In order to analytically identify different gold nanorods in a mixed condition, we fabricate a mixture, which contains nanorods with two different sizes. Fig. 2(a) shows the TEM micrograph of nanorods with two different aspect ratios, 1.6 and 3.4, respectively. The absorption spectrum of the mixed colloidal solution was measured as well, shown in Fig. 2(b), and the experimental result (the solid line) indicates that three main bands happen. The strong band with the wavelength of 750 nm is the longitudinal plasmon band of the nanorods with the aspect ratio of 3.4. The other two bands in the visible region exhibit a broad absorption at 515 nm and 570 nm, respectively.

To further realize these bands, the theoretical calculation is employed for plotting the absorption spectra of two defined nanorods, the dotted lines shown in Fig. 2(b). We found that the band at 570 nm corresponds to the longitudinal plasmon band of the nanorods with the aspect ratio of 1.6. The band at 515 nm is contributed from the transverse plasmon band of both different nanorods. Therefore, two different nanorods in a solution can be clearly and easily identified by the bands of longitudinal plasmon mode in the absorption spectrum from the experimental and theoretical analysis. The procedure can be applied even for a mixture of triple nanorods with different aspect ratios. For the applications of multiplexing targeting by using gold nanorods, the relationship between the band wavelength and the aspect ratio is the main factor. The experimental and theoretical results are shown in Fig. 3 by closed squares and solid line, respectively. The surrounding of the nanorods is regarded as water. The tunability of band wavelength extends from visible to NIR region depending on the longitudinal absorption band of different aspect ratios, and also provides the diverse selectivity for different applications.

## Plasmonic sensing measurement of C₁₆TAB solution

The plasmonic sensing experiment of the gold nanorods was performed by measuring the variations of the $C_{16}TAB$ concentration in water. The original solution was colloidal gold nanorods at a fixed concentration (30 μg mL⁻¹) in the water. Two different $C_{16}TAB$
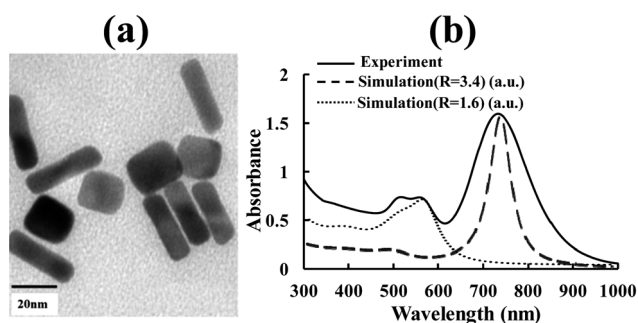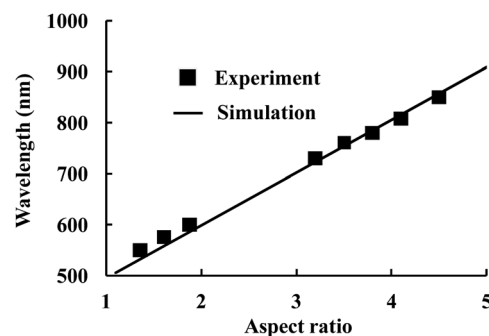


Fig. 3 The relationship of the band wavelength and the aspect ratio. The experimental results are the squares, and theoretical result is the solid line.

concentrations of 10 mM and 100 mM were added, and the dynamic changes were detected by monitoring the band shifts of LSPR in the absorption spectrum. The spectrum resolution of the instrument is 0.025 nm. Fig. 4 illustrates the effect of two $C_{16}TAB$ concentrations with the time evolution. The original band wavelength is 761.1 nm. For the case of the lower concentration (10 mM) (the squares with the solid line), a red-shift of 3 nm is observed at one minute after the $C_{16}TAB$ is mixed into the solution. Then, the blue-shift soon occurs within 10 minutes, and the band wavelength decreases to 762.4 nm after one hour. For the case of higher concentration (100 mM) (the circles with the dashed line), a red-shift of 1.4 nm happens after one minute, and the band wavelength continuously increases to 763.4 nm after one hour.

The two results exhibit the extreme difference in the time-resolved measurement, which implies that distinct mechanisms may involve. In the present solution, two major phenomena are simultaneously contributed. One is the diffusion process of $C_{16}TAB$ molecules, and the other is the physical adsorption process of $C_{16}TAB$ molecules on the gold nanorods. For the role of $C_{16}TAB$ molecule, it behaves as both the source of anisotropic growth and the stabilizer during the preparation of gold nanorods.[28] When the growth reaction stops, $C_{16}TAB$ molecules for the surface protection strongly attach to the nanorod surface, where $C_{16}TAB$ is thought to form a cationic bilayer. Since the thickness of the $C_{16}TAB$ bilayer is only a few nm, the sensing range of LSPR includes both $C_{16}TAB$ film and surrounding solution. For the case of lower concentration (10 mM), the diffusion



Fig. 2 (a) A TEM micrograph of gold nanorods mixed with two different sizes. (b) Absorption spectra of the gold nanorods with two different sizes. The solid line is the experimental result, and the dotted lines are the simulation results of the aspect ratio of 3.4 (long dots) and 1.6 (short dots).
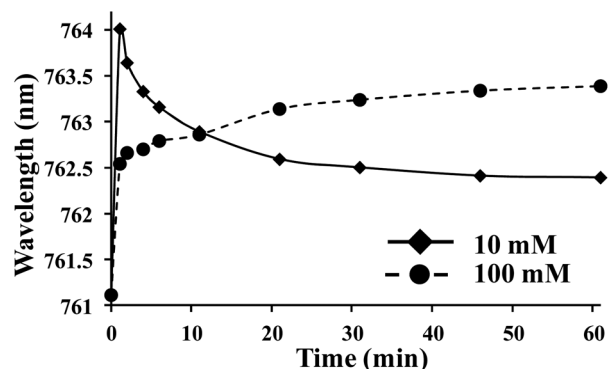


Fig. 4 The effects of different $C_{16}TAB$ concentrations, 10 mM and 100 mM. The band wavelength was measured with time.
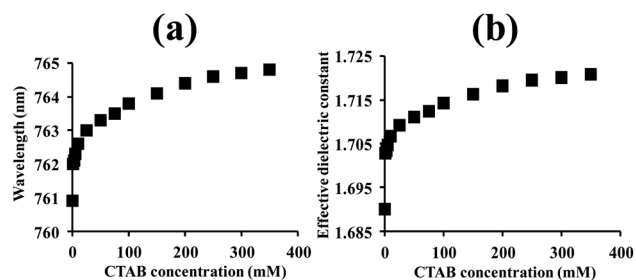
**Fig. 5** (a) The relationship of band wavelength and $C_{16}TAB$ concentration in the stationary state. (b) The relationship of effective dielectric constant and $C_{16}TAB$ concentrations.

process of $C_{16}TAB$ molecules is fast and dominant within one minute, which leads to a red-shift in the absorption spectrum. The physical adsorption slowly happens at the same time, where the $C_{16}TAB$ molecules continuously cover most of the surface of nanorods. The blue-shift from one minute later indicates that the $C_{16}TAB$ concentration in the solution decreases due to the $C_{16}TAB$ loss owing to the binding reaction on the nanorod surface. For the case of higher concentration (100 mM), the diffusion process slows down and the adsorption becomes dominant, resulting in a gradual increase of the band wavelength. After one hour, two cases reach to a stationary state, as indicated from the saturation of the $C_{16}TAB$ molecules on the nanorod surface. The difference of two band wavelengths at a stationary state between two concentrations means the different accumulated $C_{16}TAB$ thicknesses on the nanorods and concentration of $C_{16}TAB$ molecules in the solutions.

Fig. 5(a) shows the relationship of the band wavelength and $C_{16}TAB$ concentration in the stationary state. The $C_{16}TAB$ saturation concentration for the saturation condition is found higher than 400 mM. We also calculated the "effective" dielectric constants of the environment in the optical frequency (shown in Fig. 5(b)), which are contributed by the $C_{16}TAB$ molecules both on the nanorod and in the solution. These results will provide valuable information to the design of optical sensing systems.

## Conclusions

We have successfully demonstrated the plasmonic sensing technique for monitoring the variation of $C_{16}TAB$ concentration in the solution. On the basis of a simple, analytical calculation, the aspect ratio of a gold nanorod can be examined by fitting the absorption spectrum. The effective dielectric constants can be easily estimated as well. In particular, we clearly can unravel the separate mechanisms of the diffusion process of $C_{16}TAB$ molecules in the solution and the physical adsorption of $C_{16}TAB$ molecules on the nanorods. Accordingly, the utilization of gold nanorods in the plasmonic sensing technique is expected to be beneficial to investigate the chemical mixing or reaction process, and the biological interaction in a small area.

## Acknowledgements

## Notes and references

1 H. Siedentopf and R. Zsigmondy, *Ann. Phys.*, 1903, **10**, 1.
2 G. Mie, *Ann. Phys.*, 1908, **25**, 377.
3 T. R. Jensen, M. Duval Malinsky, C. L. Haynes and R. P. Van Duyne, *J. Phys. Chem. B*, 2000, **104**, 10549.
4 T. R. Jensen, M. L. Duval, K. Lance Kelly, A. A. Lazarides, G. C. Schatz and R. P. Van Duyne, *J. Phys. Chem. B*, 1999, **103**, 9846.
5 J. N. Anker, W. Paige Hall, O. Lyandres, N. C. Shah, J. Zhao and R. P. Van Duyne, *Nat. Mater.*, 2008, **7**, 442.
6 J. B. Jackson and N. J. Halas, *Proc. Natl. Acad. Sci. U. S. A.*, 2004, **101**, 17930.
7 S. Nie and S. R. Emory, *Science*, 1997, **275**, 1102.
8 K. Li, X. Li, M. Stockman and D. Bergman, *Phys. Rev. B: Condens. Matter Mater. Phys.*, 2005, **71**, 115409.
9 A. D. McFarland and R. P. Van Duyne, *Nano Lett.*, 2003, **3**, 1057.
10 G. Raschke, S. Kowarik, T. Franzl, C. Sönnichsen, T. A. Klar, J. Feldmann, A. Nichtl and K. Kürzinger, *Nano Lett.*, 2003, **3**, 935.
11 X. H. N. Xu, W. J. Brownlow, S. V. Kyriacou, Q. Wan and J. J. Viola, *Biochemistry*, 2004, **43**, 10400.
12 K.-H. Su, Q.-H. Wei, X. Zhang, J. J. Mock, D. R. Smith and S. Schultz, *Nano Lett.*, 2003, **3**, 1087.
13 W. Rechberger, A. Hohenau, A. Leitner, J. R. Krenn, B. Lamprecht and F. R. Aussenegg, *Opt. Commun.*, 2003, **220**, 137–141.
14 Q. H. Wei, K. H. Su, S. Durant and X. Zhang, *Nano Lett.*, 2004, **4**, 1067.
15 C. Sonnichsen, B. M. Reinhard, J. Liphardt and A. P. Alivisatos, *Nat. Biotechnol.*, 2005, **23**, 741.
16 S. Link and M. A. El-Sayed, *Int. Rev. Phys. Chem.*, 2000, **19**, 409.
17 K. J. Lee, P. D. Nallathamby, L. M. Browning, C. J. Osgood and X. H. N. Xu, *ACS Nano*, 2007, **1**, 133.
18 T. A. Larson, J. Bankson, J. Aaron and K. Sokolov, *Nanotechnology*, 2007, **18**, 1.
19 K. M. Mayer, S. Lee, H. Liao, B. C. Rostro, A. Fuentes, P. T. Scully, C. L. Nehl and J. H. Hafner, *ACS Nano*, 2008, **2**, 687.
20 A. Agarwal, S. W. Huang, M. O'Donnell, K. C. Day, M. Day, N. Kotov and S. Ashkenazi, *J. Appl. Phys.*, 2007, **102**, 064701.
21 E. B. Dickerson, E. C. Dreaden, X. Huang, I. H. El-Sayed, H. Chu, S. Pushpanketh, J. F. McDonald and M. A. El-Sayed, *Cancer Lett.*, 2008, **269**, 57.
22 C. Yu and J. Irudayaraj, *Anal. Chem.*, 2007, **79**, 572.
23 K. Mitamura, T. Imae, N. Saito and O. Takai, *J. Phys. Chem. B*, 2007, **111**, 8891.
24 X. Zhang and T. Imae, *J. Phys. Chem. C*, 2009, **113**, 5947.
25 S. Kawata, in *Near-field Optics and Surface Plasmon Polaritons*, ed. Springer, Berlin, 2001, pp. 97–100.
26 P. B. Johnson and R. W. Christy, *Phys. Rev. B: Solid State*, 1972, **6**, 4370.
27 G. C. Papavassiliou, *Prog. Solid State Chem.*, 1980, **12**, 185.
28 C. J. Murphy, T. K. Sau, A. M. Gole, C. J. Orendorff, J. Gao, L. Gou, S. E. Hunyadi and T. Li, *J. Phys. Chem. B*, 2005, **109**, 13857.